Reassembly and Test of High-Field Nb_3Sn Dipole Demonstrator MDPCT1

A.V. Zlobin, I. Novitski, E. Barzi, M. Baldini, J. Carmichael, S. Caspi, V.V. Kashikhin, S. Krave, C. Orozco, D. Schoerling, S. Stoynev, D. Tommasini, D. Turrioni

***Abstract*— In the framework of the U.S. Magnet Development Program (MDP), Fermilab has developed and tested a high-field Nb_3Sn dipole demonstrator MDPCT1 for a post-LHC Hadron Collider. The magnet was first assembled with a lower coil pre-load to minimize the risk of coil damage during assembly and test. In the first test the magnet reached its test goal producing a world record field of 14.1 T at 4.5 K. Next the magnet was reassembled with nominal pre-load to achieve its design field limit of 15 T. This paper describes the details of MDPCT1 inspection, design modifications and reassembly. The magnet quench performance, including training, ramp rate and temperature dependences in the temperature range of 1.9-4.5 K, is presented and discussed.**

***Index Terms*— coil pre-stress, dipole magnet, mechanical structure, Nb_3Sn superconductor, Rutherford cable, quench performance, training**

I. Introduction

FERMILAB, in the framework of the U.S. Magnet Development Program (MDP) [1], has developed a high-field Nb_3Sn dipole demonstrator MDPCT1 for a post-LHC very high energy hadron collider [2]. The main goals of this work were demonstration of a field level suitable for a future hadron collider, and study of the high-field Nb_3Sn magnet behavior, including quench performance, operation margins, field quality, and quench protection.

The magnet design is based on a 60-mm aperture 4-layer shell-type coil, graded between the inner and outer layers to maximize the magnet performance. The Rutherford cable in the two innermost coil layers has 28 strands 1.0 mm in diameter and the cable in the two outermost layers has 40 strands 0.7 mm in diameter. An innovative mechanical structure based on aluminum clamps and a thick stainless steel skin was developed to pre-load brittle Nb_3Sn coils and support large Lorentz forces at high fields. The coil axial motion under Lorentz forces is controlled by thick end plates connected by eight stainless steel rods. The 3D model and the main magnet components are shown in Fig. 1.

The conductor limits of this magnet design are 16.7 T at 1.9 K and 15.2 T at 4.5 K [2]. However, based on the mechanical analysis, the maximum field for the magnet is limited to 15 T. At higher magnetic fields, to avoid separation between pole turns and poles in the innermost layer, the coils pre-stress need to be above the safe limit for Nb_3Sn cable. When starting this program, the maximum field achieved by Nb_3Sn dipole models was limited to 13.8 T [3]. Later FRESCA2 at CERN reached 14.6 T [4].

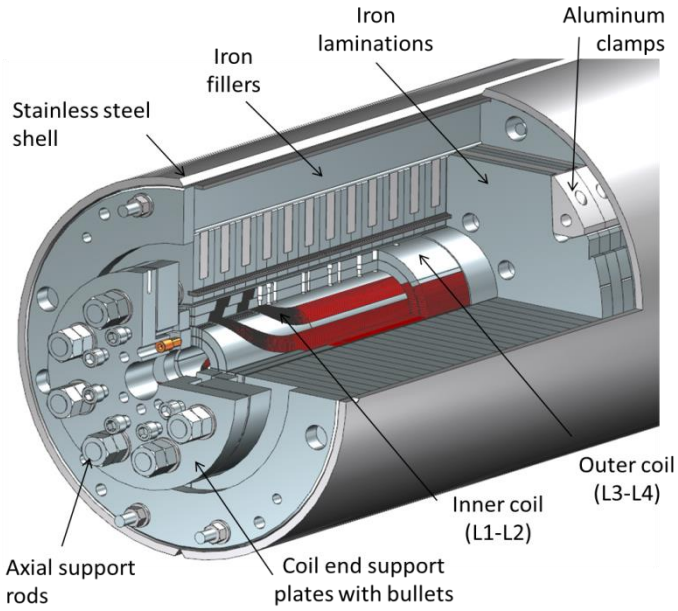

Fig. 1. Magnet design concept.

II. Magnet Fabrication and First Test Summary

The cables used in this magnet were developed and fabricated at Fermilab [5, 6] using RRP Nb_3Sn composite wires produced by Bruker-OST. Three inner-layer (IL) and three outer-layer (OL) coils were wound, reacted and epoxy impregnated. To control the reproducibility of the coil reaction cycles and estimate the magnet conductor limit, several witness samples were reacted together with each coil and tested. There was a good reproducibility of witness sample data for both inner and outer coils. Magnet conductor limits based on the witness samples are 15.2 T and 16.8 T at 4.5 K and 1.9 K respectively. They are consistent with the magnet design conductor limits.

Manuscript received October 25, 2020. This work was supported by Fermi Research Alliance, LLC, under contract No. DE-AC02-07CH11359 with the U.S. Department and US-MDP.

E. Barzi, J. Carmichael, M. Baldini, V.V. Kashikhin, I. Novitski, S. Krave, C. Orozco, S. Stoynev, D. Turrioni, A.V. Zlobin are with Fermi National Accelerator Laboratory (FNAL), P.O. Box 500, Batavia, IL 60510, USA, (phone: 630-840-8192; fax: 630-840-8079, zlobin@fnal.gov).

S. Caspi is with Lawrence Berkeley National Laboratory (LBNL), Berkeley, CA 94720-8203 USA (s_caspi@lbl.gov).

D. Schoerling, D. Tommasini are with the European Organization for Nuclear Research (CERN), Geneva 1211, Switzerland (Daniel.Schoerling@cern.ch).

Color versions of one or more of the figures in this paper are available online at http://ieeexplore.ieee.org.

Digital Object Identifier will be inserted here upon acceptance.

Template version 8.0d, 22 August 2017. IEEE will put copyright information in this area
See http://www.ieee.org/publications_standards/publications/rights/index.html for more information.

This manuscript has been authored by Fermi Research Alliance, LLC under Contract No. DE-AC02-07CH11359 with the U.S. Department of Energy, Office of Science, Office of High Energy Physics.

To determine the mechanical limits of the design, detailed FEA was performed [7, 8], and several mechanical models were assembled to test iron laminations, aluminum clamps, and preload uniformity [9]. Based on the FEA, the maximum field for this magnet is limited to 15 T due to high mechanical stress in the coil, needed to avoid pole turn separation. To minimize the risk of coil damage during assembly, it was decided to test the magnet in two steps: first with the maximum pre-stress limited to 150 MPa, which corresponds to 14 T in the magnet bore, and then with the nominal pre-stress required to achieve the design limit of 15 T.

The design and fabrication details of the Nb_3Sn dipole demonstrator, called also MDPCT1 (Magnet Development Program Cos-Theta model 1), and the results of magnet training and magnetic measurements in the first test run are reported in [10-12]. The MDPCT1 parameters are summarized in Table I.

The magnet was tested at Fermilab's Vertical Magnet Test Facility (VMTF) for the first time in May-July 2019. MDPCT1 was heavily instrumented to control electrical, mechanical and magnetic parameters. The magnet training was performed at 1.9 K to the target field of 14 T. Most quenches were detected in outer coils 4 and 5, and only two quenches were in inner coil 2. The final quench, made at 4.5 K to check conductor degradation, was at a B_{max} of 14.1 T, which confirmed that the magnet did not reach its conductor limit.

TABLE I:
MDPCT1 PARAMETERS

Parameter	Value
Magnet aperture	60 mm
Magnet outer diameter	612 mm
Coil length	1055 mm
Geometrical length including splice box	1.46 m
Total magnet weight	2390 kg
Short sample bore field B_{ssl} at 4.5 K	15.2 T
Short sample bore field B_{ssl} at 1.9 K	16.8 T

III. .MAGNET REASSEMBLY AND MODIFICATIONS

From August 2019 until February 2020 the magnet was reassembled and prepared for the new test. The magnet skin was cut in the workshop. Then the magnet was disassembled to the level of individual coils, and all the key structural components were inspected. The aluminum clamps were tested with the dye penetration technique (also known as the Liquid Penetrant Testing), and the iron laminations were tested using magnetic powder to detect possible mechanical damages. No microcracks were found in the clamps and in the yoke laminations. No visible damages were seen in the inner coils. However, noticeable coil-pole gaps in both layers of the outer coil ends were observed. This pointed at the large end motion due to insufficient axial support of the outer coils. Moreover, due to the large end motion, the outer coils have lost all the strain gauges and voltage taps traces.

The outer coil voltage tap traces were replaced with stainless steel strips as it was done in the previous R&D magnets at Fermilab. However, it was not possible to restore the traces of the strain gauge installed on the poles of the outer coils.

To achieve the magnet test goal of 15 T, the coil azimuthal pre-load has been increased by ~20 MPa with respect to the previous test [11]. It was done by adding 50 μm thick mid-plane shims to the outer coils and a 125 μm thick radial shim around the coil block, as shown in Fig. 2. To improve the coil end support, the single end plates on each side on the magnet were replaced with double plates. This allowed taking into account the different axial thermal contraction of the inner and the outer coils and providing their independent support. The outer end plates are 50 mm thick with ~120 mm ID hole. The inner coil end plates are 30 mm thick outside and 50 mm thick inside the bore of the outer coil end plates. Each pair of the inner and the outer coil support plates were independently connected by four rods as shown in Fig. 3.

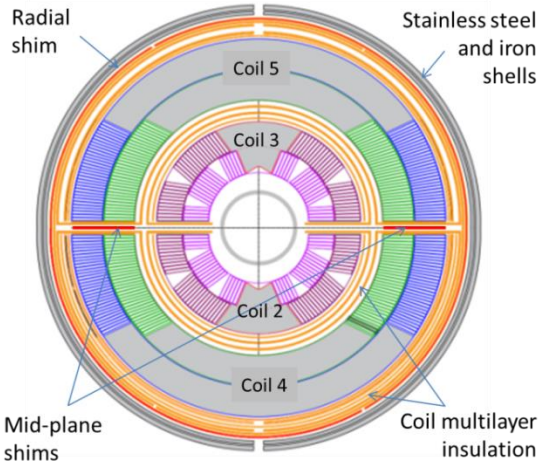

Fig. 2. The coil block cross-section and the shimming scheme.

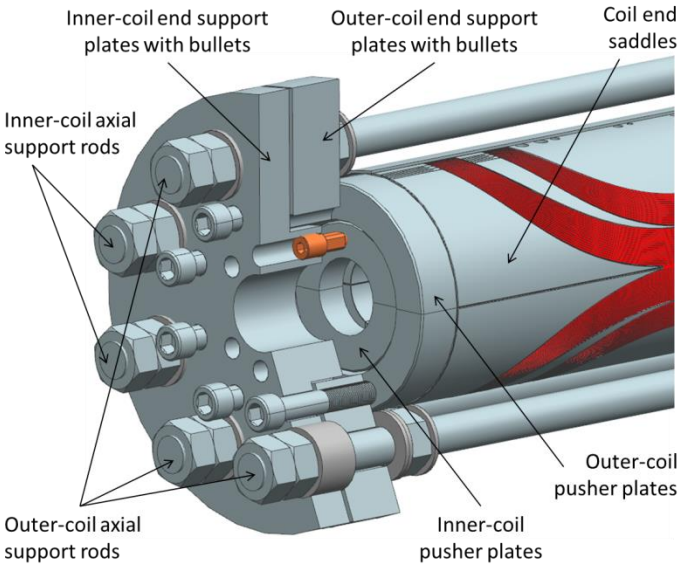

Fig. 3. New coil end support design and arrangement.

After reassembly, the magnet was connected to the VMTF Top Plate with current leads and instrumentation cables. An anti-cryostat ("warm finger") with quench antenna coils and thermometers, as well as rotating coils inside for magnetic measurements, was placed into the magnet bore. This time several acoustic gauges were also installed on the iron laminations at both ends. The magnet being prepared for installation in the VMTF cryostat is shown in Fig. 4.

Fig. 4. MDPCT1b preparation to test at VMTF.

IV. MDPCT1B TEST

After reassembly the magnet was tested in two test runs, called 2nd and 3rd test, with a warm up-cooling down cycle in between.

A. *The 2nd test*

The 2nd magnet test was performed in May-July of 2020. The main goal of this test was to achieve the design field of 15 T in the magnet aperture.

Magnet training in the 2nd test at 1.9 K is shown in Fig. 5. For comparison the magnet training in the 1st test is also presented in this and in the following plots. All the quenches in the 2nd test were detected only in outer coils 4 and 5, ~75% of all the quenches were in coil 5 and the rest in coil 4, with 64% of all the training quenches in the pole turn of the lead end. It is interesting that in the 2nd test no quenches were detected in inner coils 2 and 3, even with the increased coil pre-load and altered end support after magnet reassembly. Most of the quenches in coil 5 (78%) were recorded in the coil inner layer. The origin of these quenches, which was spread over large area at the beginning of magnet training, moved to the straight-section pole turn at the training end. 60% of the quenches in coil 4 were also detected in its inner layer. The last erratic quenches were detected in the straight section part of coil 5 inner layer close to the non-lead end.

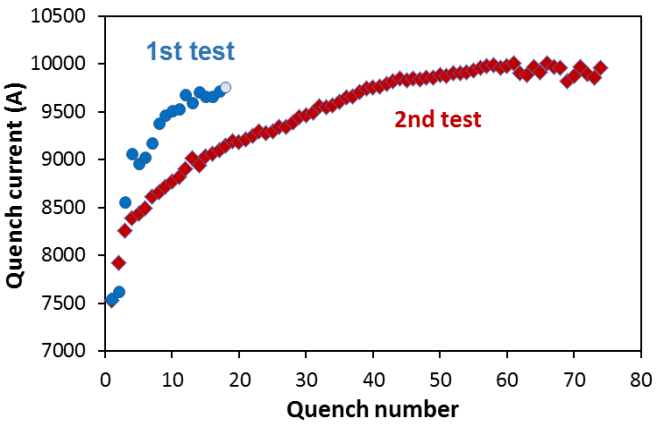

Fig. 5. MDPCT1 quench current training in the 1st and 2nd tests.

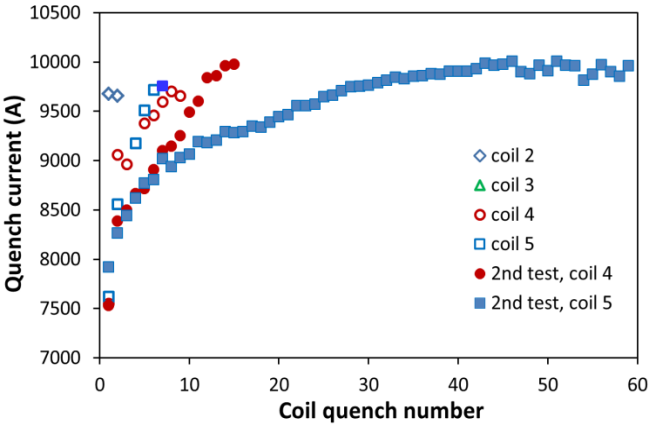

Fig. 6. Quench current sequence for each MDPCT1 coil in the 1st and 2nd tests.

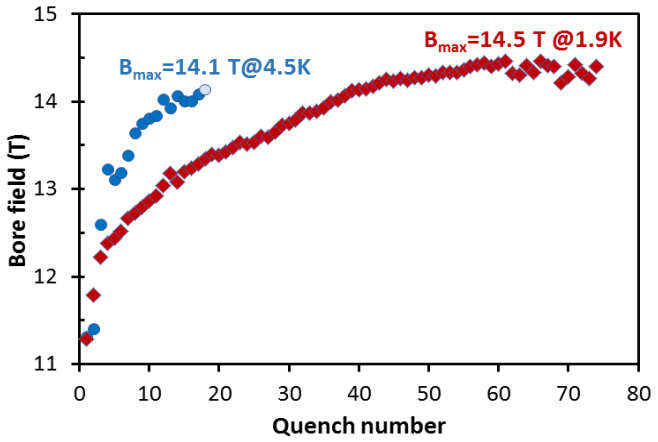

Fig. 7. Bore field vs magnet quench number in the 1st and 2nd tests.

Quench current sequences for each MDPCT1coil in the 1st and 2nd tests are plotted in Fig. 6. The first four quenches were similar in both tests. Then the training rate in the 2nd test gradually slowed down in coil 5, whereas the training rate of coil 4 was practically the same as in the 1st test. After sixty quenches the magnet training reached its maximum current and became erratic with some signs of small quench current detraining.

Fig. 7 shows training of the magnet bore field in MDPCT1 1st and 2nd tests, calculated using the data plotted in Fig. 5 and the measured magnet Transfer Function (TF) reported in [12,

13]. As mentioned above, the maximum field achieved in the 1st test at 4.5 K was 14.1 T. In the 2nd test the maximum bore field, reached during magnet training at 1.9 K, was 14.5 T. Both field values correspond to the maximum field in the magnet center. The measurements of the TF variation along the magnet axis [13] show that the bore field reaches its maximum near the coil ends (see Fig. 8), which is consistent with the 3D magnetic analysis [8]. On these bases, the maximum bore field B_{max} at 1.9 K in the aperture near the coil non-lead end corresponds to 14.6 T and the average maximum bore field between the two peaks near the coil ends is 14.53 T.

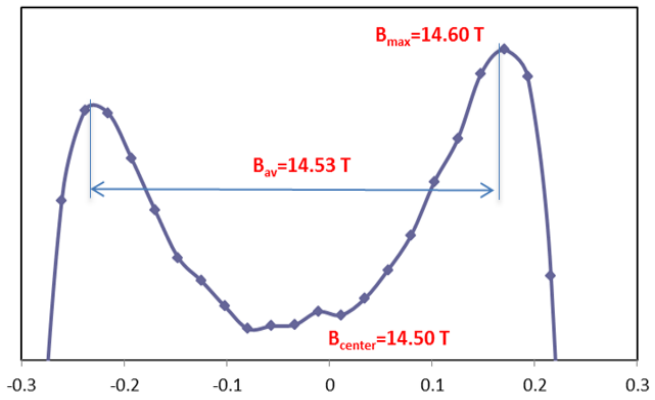

Fig. 8. Maximum bore field variation along the coil axis.

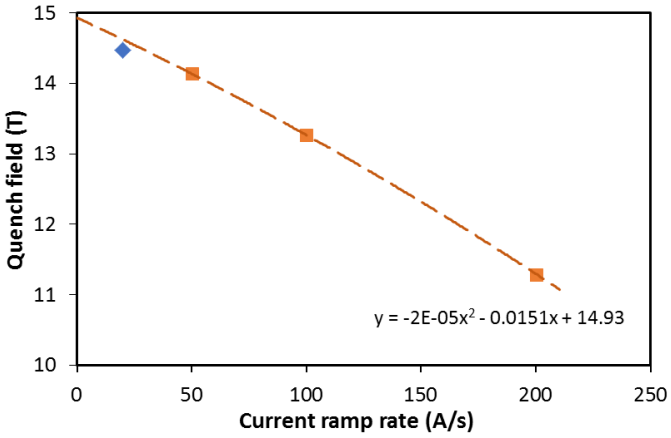

Fig. 9. Bore field vs. current ramp rate. The point at 20 A/s corresponds to the maximum bore field achieved during magnet training.

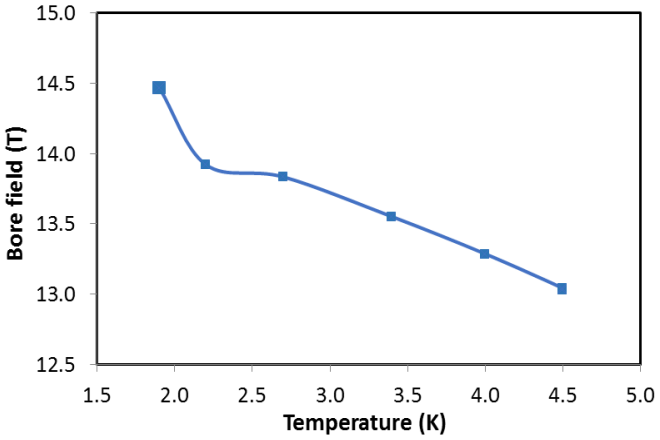

Fig. 10. Bore field vs. helium temperature. The point at 1.9 K corresponds to the maximum bore field achieved during magnet training.

Figs. 9 and 10 show the ramp rate and temperature dependences of the magnet quench bore field as measured in the 2nd test. These dependences were measured after magnet training. In both tests all the quenches were in the inner layer of coil 5.

The quenches at 50 A/s and higher ramp rates were detected in the inner layer non-lead end of coil 5. As discussed above, the low ramp rate quench started in the magnet straight section of this same coil close to the non-lead end. The fitting function was plotted based on the high ramp rate quenches, which are determined by the conductor critical current at the given ramp rate. Extrapolation of this fit to the low ramp rates shows that the magnet reached its conductor limit during training.

In the temperature dependence studies the quenches at 2.2 K and higher temperatures started in the inner-layer non-lead end of coil 5. The 1.9 K point corresponds to the highest quench current during the magnet training which started in the inner-layer straight section of coil 5 close to the non-lead end. The ramp rate and temperature dependence data show that the magnet was trained to its conductor limit as determined by the non-lead end pole turn of coil 5.

B. The 3rd test

The 3rd test was performed in August 2020 after the magnet natural warm up to ~270 K and then, without removing it from the cryostat, its slow cool down to helium temperatures. The goal of the 3rd test was to see the magnet retraining (if any) and achieve a field level in the magnet aperture close to the previous result of 14.5 T at 1.9 K.

However, no retraining was observed neither at 1.9 K nor at 4.5 K. In several consequent quenches at the same temperature the magnet demonstrated good reproducibility of quench current values, i.e. 7824±10 A at 1.9 K and 7030±5 A at 4.5 K, which corresponds to a bore field of 11.67±0.01 T and of 10.67±0.01 T respectively. Stable reproducible quench currents indicate that the magnet reached its conductor limit at both temperatures with a degradation of 18% with respect to the 2nd test. All the quenches in this test were detected in the non-lead pole turn of coil 5.

A large mechanical event was detected by the acoustic gauges in the first current ramp of the 3rd test. This event did not quench the magnet, but its longitudinal position is consistent with the locations of the performance limiting quenches. One could suggest that it may have caused the large conductor degradation observed in the 3rd test. Significant nonlinear resistance increase with current was also observed in the quenching segments in 3rd test. Signs of this mechanical event will be looked for after magnet disassembly and inspection.

C. Coil RRR measurements

The coil Residual Resistivity Ratio (*RRR*) data were collected during magnet warming up after all the three tests. Since many voltage taps were lost in the 1st test, the *RRR* values were measured only for the entire coils and were 259 and 249 for inner coils 2 and 3, and 95 and 81 for outer coils 4 and 5. In the 2nd and 3rd tests the *RRR* values were measured for each coil segment with voltage taps. The results for the 3rd test are

shown in Fig. 11. Except for the four segments in coil 3, there is good uniformity of the cable *RRR* in the various coil segments and excellent repeatability in all the three tests. These numbers are in a good agreement with the corresponding witness sample measurements.

In average the *RRR* values of the outer coils are lower than the inner coil *RRR* values. This is due to the smaller strand diameter in the outer coils (0.7 mm vs. 1 mm). The smaller strands have thinner diffusion barrier which allows more tin leakages to the strand copper matrix during coil reaction.

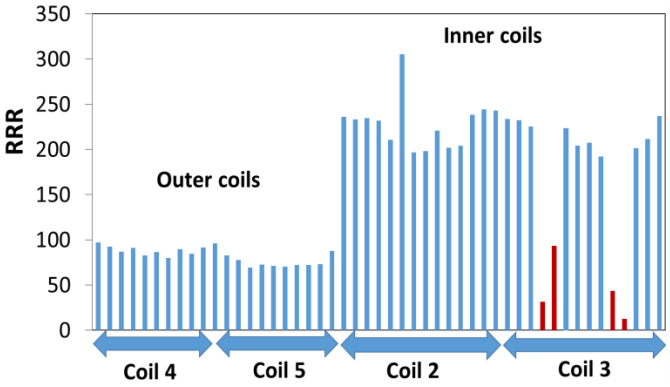

Fig. 11. *RRR* values in the inner and outer coils after the 3rd test. The low values in red color are due to technical issues for some readings.

V. Summary and Conclusions

The high-field Nb_3Sn dipole demonstrator MDPCT1 for a post-LHC hadron collider was developed and tested at Fermilab. This work was an important MDP milestone to understand the limits of the state-of-the-art Nb_3Sn accelerator magnet technology. During 2019-2020 the magnet was tested in three test runs over a temperature range from 1.9 K to 4.5 K. The performance limits of the magnet design and the magnet test results are summarized in Fig. 12. In the 1st test the magnet bore field has reached 14.1 T at 4.5 K and in the 2nd test 14.5 T at 1.9 K. These two results establish two new world records for accelerator magnets.

Although the maximum bore field, achieved in the 2nd test, slightly increased at 1.9 K, there is 8% performance degradation at 4.5 K with respect to the magnet 1st test, and even larger performance degradation was observed in the 3rd test after a thermal cycle. This result is quite surprising since the magnet was not removed from the cryostat and the warming up and cooling down procedures were slow and well controlled.

The magnet performance in all the tests was limited by the outer coils, and in the last two tests only by coil 5. The test data show that the magnet was trained to its conductor limit as determined by the non-lead pole turn of coil 5. The causes of the magnet quench performance degradation are under investigation. The magnet is being disassembled and inspected; the findings and lessons learned will be reported in a special report.

The goals of this program have been achieved – the graded four-layer coil, the innovative support structure and the magnet fabrication technologies and assembly procedures were developed, and the magnet performance was tested. The maximum field reached in the 2nd test at 1.9 K is 97% of the program goal of 15 T. The 14.1 T and 14.5 T fields achieved in the MDPCT1 aperture at 4.5 K and 1.9 K respectively (together with the FRESCA2 result at 1.9 K) set new world records for the Nb_3Sn accelerator dipole magnets (see Fig. 13). Large step has been made in the Fermilab's HFM program from the initial field of ~11 T. With this test the MDPCT1 program is complete. The performance limitations, observed in MDPCT1, will be addressed using coils with stress management [15], which is a key task of the updated MDP plan [16].

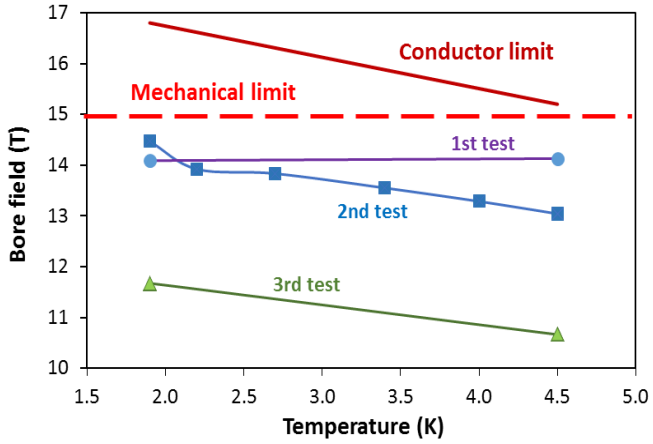

Fig. 12. Magnet maximum design field limits and measured bore fields at various temperatures.

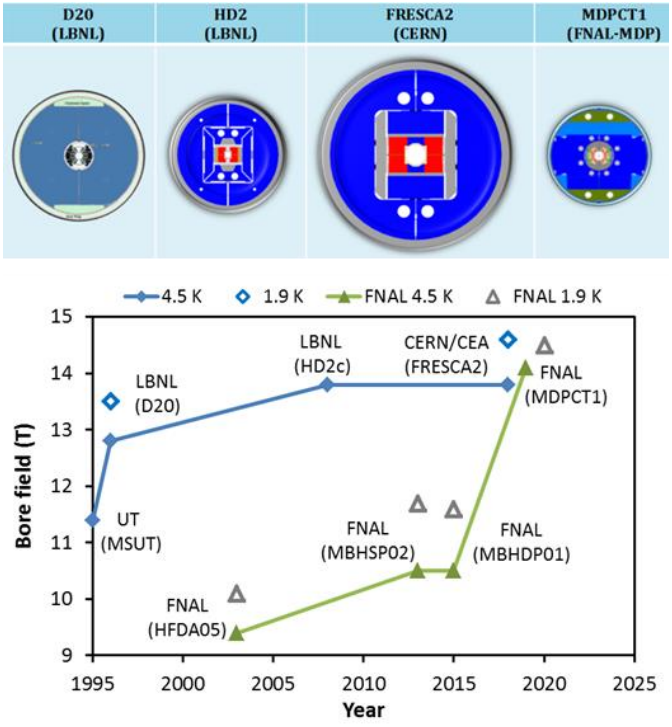

Fig. 13. Cross-sections and names of record field Nb_3Sn accelerator dipole short models (top), and progress of maximum field in Nb_3Sn accelerator dipoles worldwide and at Fermilab during 1995-2020 (bottom). The plot is based on the data presented in [14].

ACKNOWLEDGMENT

The authors thank technical staff of FNAL, LBNL and CERN for contributions to the magnet design, fabrication and test, and the US-MDP Management Group and Technical Advisory Committee for support of this project. Special thanks to Jodi A. Coghill for her key contribution to the magnet part design and to Allen Rusy and James Karambis for their valuable role in the magnet reassembly and production tests.

REFERENCES

[1] S. Gourlay, A.V. Zlobin, S. Prestemon, D.C. Larbalestier, and L. Cooley, "The U.S. magnet development program plan," 16-AT-2934, LBNL-100646, Berkeley, CA, USA, June 2016.

[2] A.V. Zlobin, N. Andreev, E. Barzi, V.V. Kashikhin, I. Novitski, "Design concept and parameters of a 15 T Nb_3Sn dipole demonstrator for a 100 TeV hadron collider", Proc. of IPAC2015, Richmond, VA, USA, p.3365.

[3] P. Ferracin, B. Bingham, S. Caspi et al., "Assembly and test of HD2, a 36 mm bore high field Nb_3Sn dipole magnet," *IEEE Trans. Appl. Supercond.*, Vol. 19, Issue 3, June 2009, pp. 1240–1243.

[4] G. Willering, C. Petrone, M. Bajko et al., "Cold powering tests and protection studies of the FRESCA2 100 mm bore Nb_3Sn block-coil magnet," *IEEE Trans. Appl. Supercond.*, Vol. 28, Issue 3, April 2018, Art.no. 4005105.

[5] E. Barzi, N. Andreev, P. Li, V. Lombardo, D. Turrioni, and A.V. Zlobin, "Nb_3Sn RRP® Strand and Rutherford Cable Development for a 15 T Dipole Demonstrator," *IEEE Trans. Appl. Supercond.*, Vol. 26, Issue 3, June 2016, Art.no. 4001007.

[6] E. Barzi, M. Bossert, M. Field, P. Li, H. Miao, J. Parrell, D. Turrioni, A.V. Zlobin, "Heat Treatment Optimization of Rutherford Cables for a 15 T Nb_3Sn Dipole Demonstrator", *IEEE Trans. Appl. Supercond.*, Vol. 27, Issue 4, June 2017, Art.no. 4802905.

[7] C. Kokkinos, I. Apostolidis, J. Carmichael, T. Gortsas, S. Kokkinos, K. Loukas, I. Novitski, D. Polyzos, D. Rodopoulos, D. Schoerling, D. Tommasini,.and A.V. Zlobin, "FEA Model and Mechanical Analysis of the Nb_3Sn 15 T Dipole Demonstrator," *IEEE Trans. Appl. Supercond.*, Vol. 28, Issue 3, April 2018, Art.no. 4007406.

[8] I. Novitski, N. Andreev, E. Barzi, J. Carmichael, V. V. Kashikhin, D. Turrioni, M. Yu, and A. V. Zlobin, "Development of a 15 T Nb_3Sn Accelerator Dipole Demonstrator at Fermilab", *IEEE Trans. Appl. Supercond.*, Vol. 26, Issue 3, June 2016, Art.no. 4001007.

[9] C. Orozco, J. Carmichael, I. Novitski, S. Stoynev, A.V. Zlobin, "Assembly and Tests of Mechanical Models of the 15 T Nb_3Sn Dipole Demonstrator," *IEEE Trans. Appl. Supercond.*, Vol. 29, Issue 5, August 2019, Art.no. 4003404.

[10] A.V. Zlobin, I. Novitski, E. Barzi, J. Carmichael, G. Chlachidze, J. DiMarco, V.V. Kashikhin, S. Krave, C. Orozco, S. Stoynev, T. Strauss, M. Tartaglia, D. Turrioni, "Quench performance and field quality of the 15 T Nb_3Sn dipole demonstrator MDPCT1 in the first test run", Proc. of NAPAC2019, Lansing (MI), 1-6 September 2019, paper MOPLO20.

[11] A.V. Zlobin, I. Novitski, V.V. Kashikhin, E. Barzi, J. Carmichael, S. Caspi, G. Chlachidze, S. Krave, C. Orozco, D. Schoerling, S. Stoynev, D. Tommasini, D. Turrioni, "Development and First Test of the 15 T Nb_3Sn Dipole Demonstrator MDPCT1", *IEEE Trans. Appl. Supercond.*, Vol. 30, Issue 4, 2020, Art.no. 4000805

[12] T. Strauss, E. Barzi, J. DiMarco, V.V. Kashikhin, I. Novitski, M. Tartaglia, G. Velev, A.V. Zlobin, "First field measurements of the 15 T Nb_3Sn Dipole Demonstrator MDPCT1", *IEEE Trans. Appl. Supercond.*, Vol. 30, Issue 4, 2020, Art.no. 4001106

[13] J. DiMarco, M. Baldini, E. Barzi, V.V. Kashikhin, I. Novitski, T. Strauss, M. Tartaglia, G.V. Velev, A.V. Zlobin, "Field Measurement Results of the 15 T Nb_3Sn Dipole Demonstrator," Wk1LPo1A-07, *IEEE Trans. Appl. Supercond.,* submitted for publication.

[14] Nb_3Sn Accelerator Magnets - Designs, Technologies and Performance, Editors Daniel Schoerling and Alexander V. Zlobin, Springer, 2019, https://doi.org/10.1007/978-3-030-16118-7

[15] I. Novitski, J. Carmichael, V.V. Kashikhin, and A.V. Zlobin, "High-Field Nb_3Sn Cos-theta Dipole with Stress Management," FERMILAB-CONF-17-340-TD, 2017.

[16] Soren Prestemon, Kathleen Amm, Lance Cooley, Steve Gourlay, David Larbalestier, George Velev, Alexander Zlobin, "The 2020 Updated Roadmaps for the US Magnet Development Program," 2020 arXiv:2011.09539 [physics.acc-ph].